# Reversal of the cellular phenotype in the premature aging disease Hutchinson-Gilford progeria syndrome

Paola Scaffidi & Tom Misteli

**Hutchinson-Gilford progeria syndrome (HGPS) is a childhood premature aging disease caused by a spontaneous point mutation in lamin A (encoded by *LMNA*), one of the major architectural elements of the mammalian cell nucleus[1–4]. The HGPS mutation activates an aberrant cryptic splice site in *LMNA* pre-mRNA, leading to synthesis of a truncated lamin A protein and concomitant reduction in wild-type lamin A[3,4]. Fibroblasts from individuals with HGPS have severe morphological abnormalities in nuclear envelope structure. Here we show that the cellular disease phenotype is reversible in cells from individuals with HGPS. Introduction of wild-type lamin A protein does not rescue the cellular disease symptoms. The mutant *LMNA* mRNA and lamin A protein can be efficiently eliminated by correction of the aberrant splicing event using a modified oligonucleotide targeted to the activated cryptic splice site. Upon splicing correction, HGPS fibroblasts assume normal nuclear morphology, the aberrant nuclear distribution and cellular levels of lamina-associated proteins are rescued, defects in heterochromatin-specific histone modifications are corrected and proper expression of several misregulated genes is reestablished. Our results establish proof of principle for the correction of the premature aging phenotype in individuals with HGPS.**

Hutchinson-Gilford progeria syndrome is most commonly caused by a *de novo* heterozygous silent substitution at codon 608 (G608G: GGC→GGT) of the lamin A/C (*LMNA*) gene[3,4]. The mutation resides in exon 11 of *LMNA* and activates an exonic cryptic donor splice site four nucleotides upstream. The pre-mRNA derived from the mutated allele is spliced using this aberrant donor splice site and the correct exon 12 acceptor splice site, giving rise to a truncated *LMNA* mRNA lacking the terminal 150 nucleotides of exon 11 (refs. 3,4). As a consequence of the aberrant splicing event, a mutant protein, Δ50 lamin A, containing a 50–amino acid internal deletion in its globular tail domain is generated[3,4]. Fibroblasts from individuals with HGPS are characterized by the presence of dysmorphic nuclei with altered size and shape, showing lobules, wrinkles and herniations upon staining for lamin A[3–6] (**Fig. 1a,b**). Aberrant morphology (as assessed by a nuclear envelope contour ratio of <0.7) was present in typically ~70% of cells in several HGPS cell lines (**Supplementary Table 1** online). In

addition to these well-established morphological changes, we found several hitherto unknown defects in HGPS fibroblasts. In ~70% of the cells, lamin B, lamin A's major interacting partner, and several members of the family of lamina-associated polypeptides (LAP2s) were depleted from their typical localization at the nuclear envelope, and the global cellular amount of these proteins was reduced up to sixfold compared with the control cells when assessed by total cellular fluorescence intensity measurements (**Fig 1a,b** and **Supplementary Table 1** online). Furthermore, ~60% of HGPS cells showed a reduction of at least twofold in the heterochromatin protein HP1α, one of the adaptors between the nuclear lamina and chromatin[7] (**Fig. 1a,b** and **Supplementary Table 1** online). The reduction in HP1α coincided with aberrant histone modification status of chromatin, with reduction or complete loss of the heterochromatin marker tri-methyl lysine 9 of core histone H3 (Tri-Me-K9)[8] in ~60% of the cells (**Fig. 1a,b** and **Supplementary Table 1** online). Reductions in the lamina-associated proteins, HP1α and Tri-Me-K9 in the entire cell population were confirmed by western blotting (data not shown).

Using these characteristics of fibroblasts from individuals with HGPS, we set out to ask whether the morphological and cellular changes associated with progeria are permanent or reversible. In HGPS cells the presence of the mutant lamin A is accompanied by a reduction in the amount of the wild-type protein and the cellular defects could thus be the result of either a decrease in fully functional wild-type lamin A or a dominant negative effect of the mutant Δ50 lamin A. Transfection of cells from individuals with HGPS with a plasmid simultaneously expressing untagged lamin A and green fluorescent protein (GFP) to identify transfected cells did not lower the percentage of cells with aberrant overall morphology compared to untransfected cells (**Fig. 1c** and **Supplementary Table 1** online) and was insufficient to restore the normal cellular levels of the lamina-associated proteins and HP1α (**Fig. 1c** and **Supplementary Table 1** online). Furthermore, it did not re-establish proper histone modifications in heterochromatin in HGPS cells (**Fig. 1c**; **Supplementary Table 1** online). Even high levels and prolonged expression of wild-type lamin A for up to 10 d were not effective in correcting the cellular HGPS defects (data not shown). Identical results were obtained using a FLAG-tagged and GFP-tagged lamin A, previously shown to complement lamin A–deficient cells[9–11] (data not shown). Analysis of the dynamic properties of the introduced wild-type GFP–lamin A suggested that the failure to rescue

National Cancer Institute, National Institutes of Health, 9000 Rockville Pike, Bethesda, Maryland 20892, USA. Correspondence should be addressed to T.M. (mistelit@mail.nih.gov).
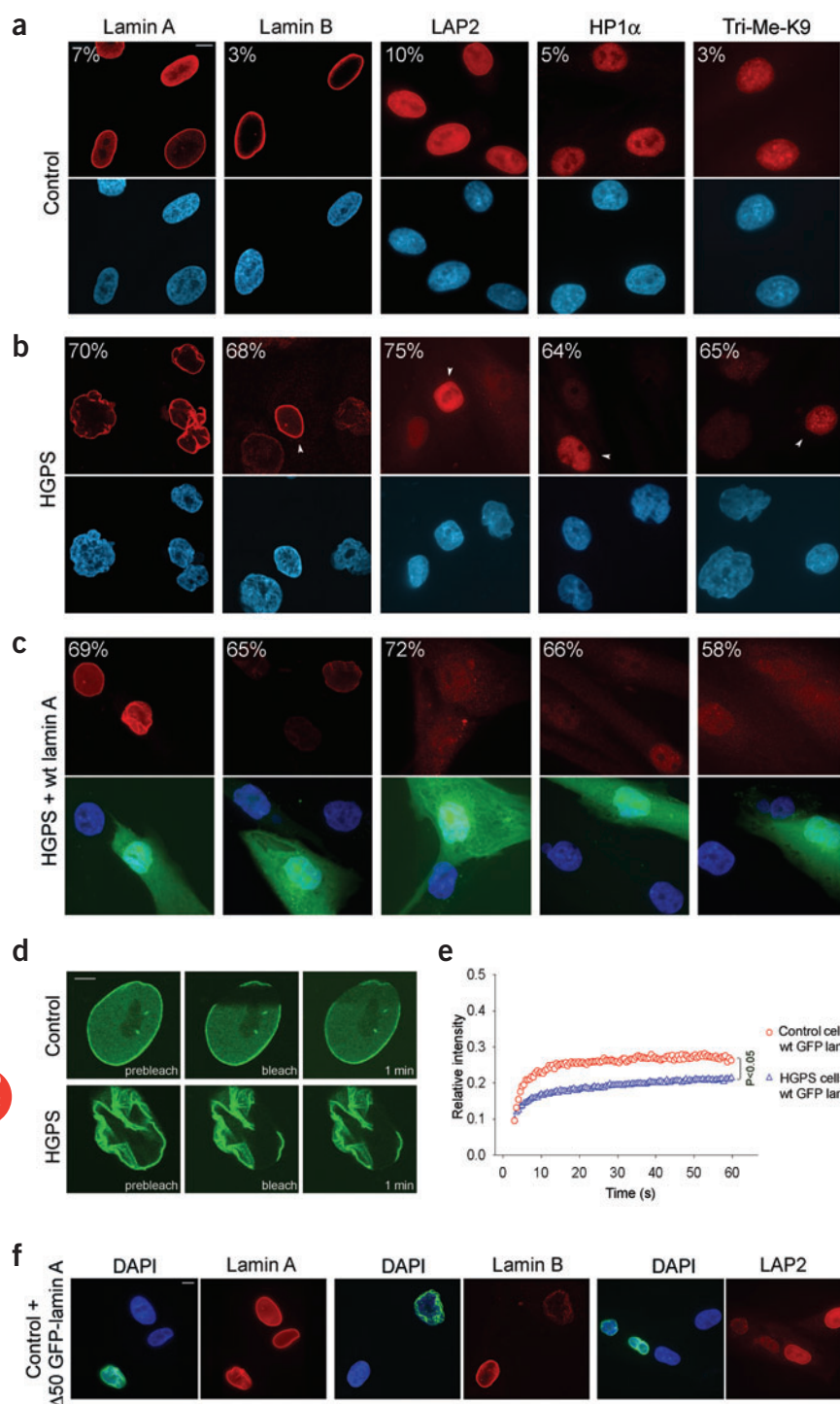
**Figure 1** Wild-type lamin A is insufficient for phenotypic rescue of HGPS cells. (**a**–**c**) Immunofluorescence microscopy on primary dermal fibroblasts from a healthy control individual (AG08469; population doublings: 25–30) (**a**) and an individual with HGPS (AG01972; population doublings: 25–30), untreated (**b**) or transfected with wild-type lamin A and GFP as a transfection marker (**c**). Cells were stained with DAPI (blue) and antibodies (red) against the indicated proteins. Cells with normal staining for lamin B, LAP2, HP1α and Tri-Me-K9, respectively, are indicated by arrowheads in **b** to directly compare the cellular level of the proteins in unaffected and affected cells. The percentage of cells showing aberrant phenotype is indicated. Scale bar, 10 μm. (**d**) FRAP analysis of wild-type GFP–lamin A in living control and HGPS cells. Nuclei were imaged before and during recovery after the bleach pulse. Scale bar, 5 μm. (**e**) Kinetics of recovery of the fluorescence signal in the entire bleached area. (**f**) Immunofluorescence microscopy on primary dermal fibroblasts from a healthy control individual (AG08469; population doublings: 25–30) transfected with GFP–Δ50 lamin A. Cells were stained with DAPI (blue) and antibodies (red) to lamin A/C, lamin B or LAP2 proteins. The green fluorescent signal from GFP–Δ50 lamin A is overlaid with the DAPI signal. Scale bar, 10 μm.

in control fibroblasts induced nuclear morphological defects similar to those observed in HGPS cells and led to a reduction in the cellular levels of lamin B and LAP2 (**Fig. 1f**).

Because of the dominant negative nature of the mutant lamin A protein, reversal of the cellular phenotype in HGPS cells requires the elimination of the mutant protein. To do so, we sought to correct the aberrant splicing of the mutant *LMNA* pre-mRNA. We designed a 25-mer morpholino oligonucleotide (exo11) complementary to the region containing the HGPS mutation in exon 11 to sterically block the activated cryptic splice site, thus preventing the access of the splicing machinery to the aberrant splice site[12] (**Fig. 2a**). In contrast to unmodified oligonucleotides, morpholinos are stable and they neither induce RNase H degradation of the heteroduplex nor interfere with translation[13,14]. The exo11 oligonucleotide was able to correct aberrant splicing of a *LMNA* minigene in HeLa cells (**Supplementary Fig. 1** online). To test

the progeria phenotype was probably because of the inability of wild-type lamin A to function properly in HGPS cells. In fluorescence recovery after photobleaching (FRAP) experiments, recovery kinetics of wild-type GFP–lamin A were reduced in HGPS cells as compared with control cells ($P < 0.05$), indicating that wild-type lamin A becomes more tightly associated with its nuclear binding sites in the presence of the mutant protein (**Fig. 1d,e**). The observation that the cellular behavior of wild-type lamin A is altered in the presence of the mutant lamin A suggests a dominant negative effect of Δ50 lamin A in HGPS cells. In support of this conclusion, expression of GFP–Δ50 lamin A

whether aberrant splicing of the endogenous *LMNA* transcript could be corrected, exo11 oligonucleotide was introduced into HGPS fibroblasts by two sequential electroporations. We analyzed the splicing pattern of endogenous lamin A after 4 d by RT-PCR, using primers in exons 9 and 12. Oligonucleotide treatment effectively blocked aberrant splicing of endogenous *LMNA* mRNA with a half-maximal effect at ~7 μM and resulted in the removal of ≤90% of the truncated *LMNA* mRNA (**Fig. 2b,c**). Similar results were obtained in three dermal fibroblast and two B-lymphocyte cell lines derived from individuals with HGPS, indicating that correction of *LMNA* aberrant splicing can be

achieved with similar efficiency in several cell types (**Fig. 2b,c**). We did not observe any change in the relative amount of splice products after treatment with a control scrambled oligonucleotide, indicating that correction of aberrant splicing occurs in an oligonucleotide sequence–specific manner (**Fig. 2b,c**). The exo11 oligonucleotide was specific for correction of the aberrant splicing event and had no effect on other splicing events in *LMNA* pre-mRNA as shown by similar RNA levels and the absence of aberrant splice products when probed along the entire mRNA (**Fig. 2d–f**). Concentrations of ≥40 µM resulted in a slight increase of lamin C production. This increase is probably the result of a partial block of the normal exon 11–intron 11 junction, which shares 16 out of 25 nucleotides with the activated splice site, resulting in the activation of the lamin C alternative splice site in exon 10 (ref. 15; **Fig. 2e,f**). In agreement with previous reports showing high sequence specificity of morpholino oligonucleotides[14,16], we saw no effect on splicing of several cellular RNAs (**Supplementary Fig. 2** online).
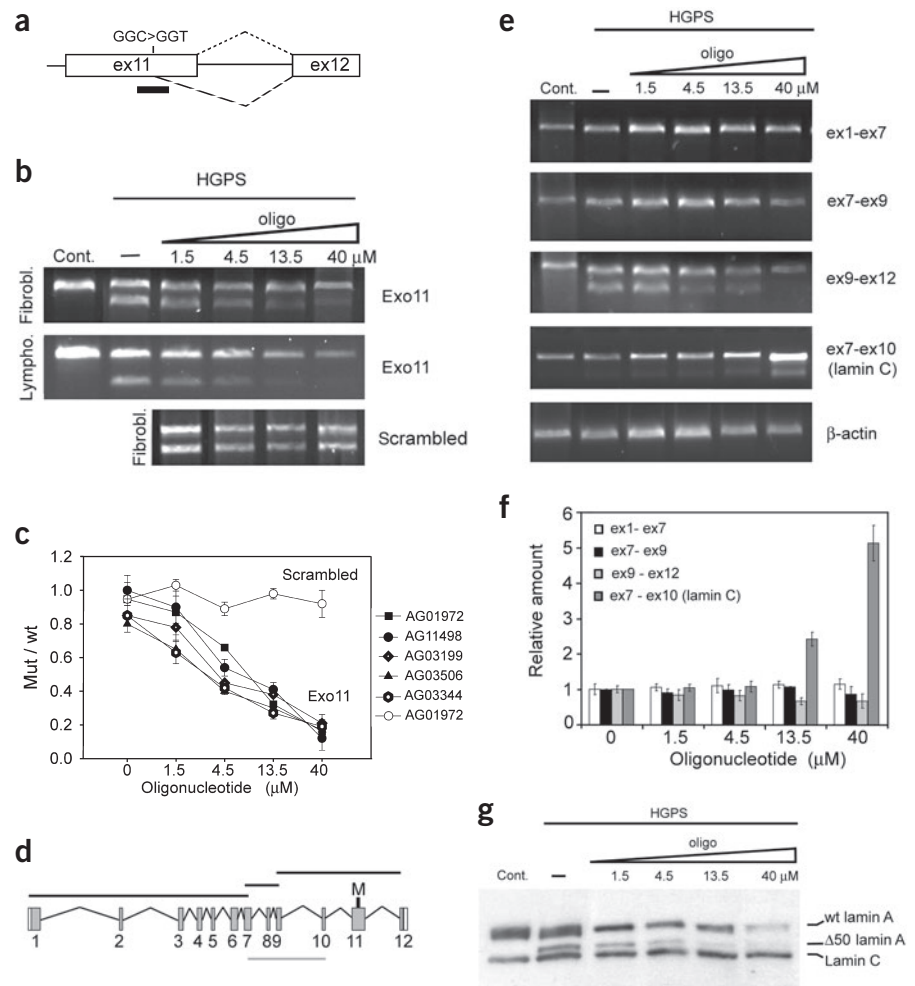
To confirm that correction of aberrant splicing of the *LMNA* pre-mRNA also resulted in a reduction of the mutant lamin A protein, we performed western blot analysis on treated fibroblasts from individuals with HGPS. Titration of exo11 oligonucleotide induced progressive reduction of mutant lamin A, leaving <5% of the protein at concentrations >13.5 µM (**Fig. 2g**). In agreement with the effects observed at the RNA level, wild-type lamin A did not increase upon treatment, and at high concentrations of oligonucleotide lamin C was moderately increased in comparison with lamin A (**Fig. 2g**).

We used several criteria to test whether correction of the splicing event restored the normal cellular phenotype in fibroblasts from individuals with HGPS. Treatment of HGPS cells with 13.5 or 40 µM exo11 oligonucleotide corrected the morphological abnormalities of cell nuclei in >90% of cells (**Fig. 3a–c; Supplementary Table 1** online). Nuclei lost the severe wrinkles, herniations and lobes typically observed in HGPS cells

and acquired a normal ellipsoid shape indistinguishable from that of control cells (contour ratio = 0.89 ± 0.1) (**Fig. 3a–c** and **Supplementary Table 1** online). The normal cellular complement of lamin B, LAP2 proteins and HP1α was restored in ~90% of treated cells (**Fig. 3a–d** and **Supplementary Table 1** online). Upon treatment, we observed normal concentrations of Tri-Me-K9 in HGPS cells (**Fig. 3a–c** and **Supplementary Table 1** online). Finally, normal cellular behavior of the wild-type lamin A protein was restored after correction of aberrant splicing. In the FRAP assay, GFP–lamin A was dynamically exchanged at similar rates in control cells and in HGPS cells treated with oligonucleotide, suggesting that correction of splicing restores proper dynamic interactions of the lamin A protein *in vivo* (**Fig. 3e,f**).

Reversal of the cellular phenotype in HGPS fibroblasts did not require mitosis or nuclear lamina disassembly. Analysis of single living cells expressing GFP–lamin A by *in vivo* imaging showed restoration of normal nuclear morphology without mitosis (**Supplementary Fig. 3** online). In addition, when cell division was prevented during oligonucleotide treatment by either contact inhibition or arrest of cells in G0, the normal cellular phenotype as assessed by lamin A, LAP2 or HP1α staining was restored in most cells (**Supplementary Fig. 3** online).

As a final criterion for restoration of normal cellular function of HGPS cells, we analyzed the expression levels of genes that are misregulated in fibroblasts from individuals with progeria. Several genes have been shown by microarray analysis to be differentially expressed
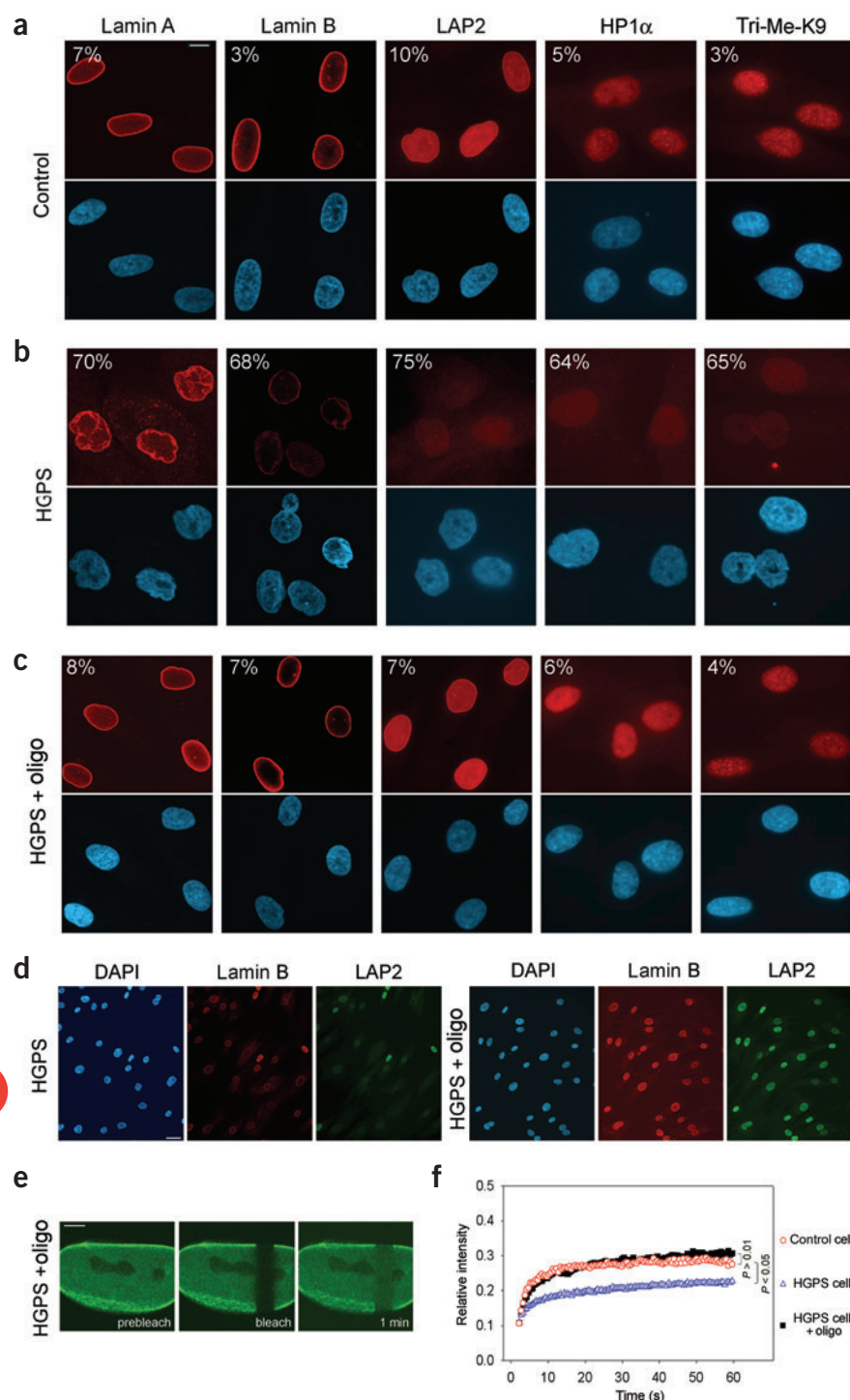


**Figure 2** Correction of aberrant splicing in the endogenous lamin A transcript in HGPS cells. (**a**) Schematic representation of the region of *LMNA* pre-mRNA targeted by exo11 antisense oligonucleotide. The predicted splicing events (dotted line, normal splicing; dashed line, aberrant splicing) and the position of exo11 oligonucleotide (black bar) are indicated. (**b**) RT-PCR analysis of control and HGPS fibroblasts and lymphocytes subjected to two sequential electroporations with oligonucleotide or mock treated. (**c**) Quantification of exo11 (black symbols) and scrambled (open symbols) oligonucleotides titration in different cell lines. All values represent averages from five independent experiments ± s.d. (**d**) Schematic representation of the different fragments of *LMNA* lamin A (black bars) and lamin C (gray bar) cDNAs amplified by RT-PCR. (**e**) RT-PCR analysis and (**f**) quantification of the indicated fragments after oligonucleotide titration. The intensity of each band was normalized to the intensity of the corresponding β-actin band. (**g**) Western blot analysis of control cells and HGPS fibroblasts subjected to three sequential electroporations with oligonucleotide or mock treated, analyzed 6 d after the first delivery.

**Figure 3** Phenotypic rescue of HGPS cells by treatment with morpholino oligonucleotide. (**a**–**d**) Immunofluorescence microscopy on primary dermal fibroblasts from a healthy control individual (**a**) and an individual with HGPS (AG01972) untreated (**b**) or treated with oligonucleotide (**c**). Cells were stained with DAPI (blue) and antibodies (red) to the indicated proteins. The percentage of cells showing aberrant phenotype is indicated. Scale bar, 10 μm. (**d**) Low-magnification images of untreated and treated HGPS cells. Scale bar, 35 μm. (**e**) FRAP analysis of wild-type GFP–lamin A in HGPS cells upon splicing correction. A nucleus was imaged before and during recovery after the bleach pulse. Scale bar, 5 μm. (**f**) Kinetics of recovery of the fluorescence signal in the entire bleached area as compared to control and untreated HGPS cells.

Expression of *CCL8* and *MMP14* was reduced and that of *TIMP3*, *MMP3* and *HAS3* was increased to levels similar to control cells. As a negative control, signal transducer and activator of transcription 3 (*STAT3*), which is unchanged by the lamin A mutation, was not affected by the presence of the oligonucleotide. These results show that correction of the aberrant splicing defect of *LMNA* premRNA restores normal expression of several genes misregulated in HGPS.

Our findings show that elimination of the mutant HGPS lamin A protein is necessary and sufficient to rescue the progeria cellular phenotype in fibroblasts from individuals with HGPS. Together with the inability to restore the normal cellular phenotype by overexpressing wild-type lamin A in HGPS cells, these data indicate that the cellular defects in cells from individuals with HGPS result from a dominant negative mode of action of the mutant lamin A protein. Furthermore, overexpression of Δ50 lamin A in wild-type cells induces abnormalities in nuclear morphology[6] (**Fig. 1f**). The observation that in HGPS cells the presence of Δ50 lamin A severely compromises the cellular behavior of wild-type lamina A and the composition of the nuclear rim is additional direct evidence for the dominant negative role of mutant lamin A.

The reversibility of the cellular disease phenotype by all tested criteria through correction of the aberrant splicing event may be used as a strategy for therapeutic purposes. The observation that cells can be rescued independently of mitosis suggests that reversal of the cellular phenotype might also be feasible in nondividing tissues. Although a mouse mutant showing several progeria symptoms[19] is available, this animal model is not suitable for further testing of our approach because its molecular basis is a L530P mutation rather than the G608G mutation found in humans and does not result in simple activation of a cryptic splice site[19]. Although morpholinos and oligonucleotides of other chemistries have successfully been used for sustained delivery in
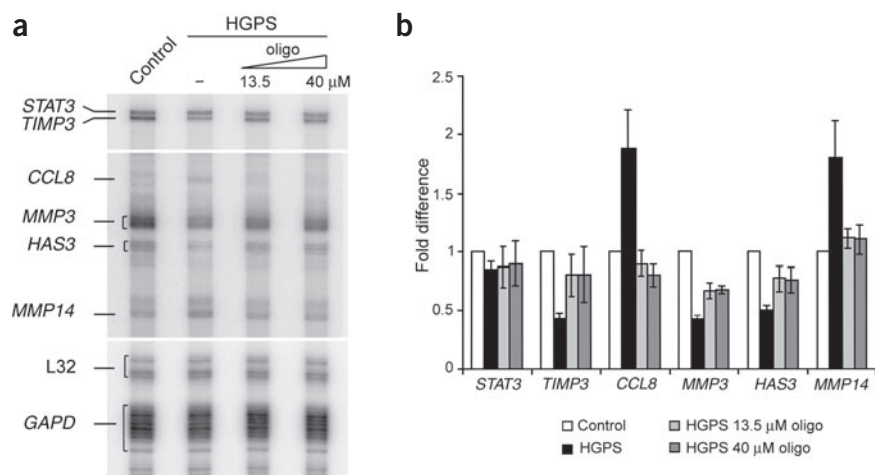
in HGPS cells[17,18]. In agreement with those results, we found by RNase protection (**Supplementary Methods** online) a twofold reduction of matrix metalloproteinase 3 (encoded by *MMP3*), hyaluron synthase III (encoded by *HAS3*) and tissue inhibitor of metalloproteinase 3 (encoded by *TIMP3*), as well as a twofold increase in matrix metalloproteinase 14 (encoded by *MMP14*) and chemokine (C-C motif) ligand 8 (encoded by *CCL8*) mRNA in HGPS cells as compared with age-matched control cells (**Fig. 4a,b**). Upon treatment of HGPS cells with oligonucleotide, the expression of all five genes returned to the levels observed in age-matched healthy control cells (**Fig. 4a,b**).

**a**



**b**

**Figure 4** Restoration of normal gene activity in HGPS cells by treatment with oligonucleotide. (**a**) RNase protection assay on control cells (CRL-1474) and HGPS cells (AG11498) subjected to three electroporations with oligonucleotide or mock treated. A longer exposure of the gel is shown for *CCL8*, *MMP3*, *HAS3* and *MMP14* because of the low expression level of those genes in comparison with *STAT3*, *TIMP3*, *MRPL32* and *GAPD*. (**b**) Quantitation of gene expression. Values represent fold differences of the indicated mRNA levels between untreated and treated HGPS cells and control cells. Values are averages from at least three independent experiments ± s.d.

animals and humans[12,20,21], splicing correction might also be achieved by use of trans-splicing expression systems as applied to other splicing diseases or by use of small-molecule inhibitors[22]. Whichever method is used, our results establish proof of principle for the reversal of the cellular effects of premature aging in progeria.

## METHODS

**Cell culture and transfection.** Primary dermal fibroblast cell lines and lymphoblastoid cell lines from persons with HGPS and healthy donors were obtained from the Aging Repository of the Coriell Cell Repository (CCR) and from the American Type Culture Collection (ATCC). HGPS fibroblast cell lines were AG01972 (patient age 14 years, CCR, PDs 22 at purchase), AG11498 (14 years, CCR, PDs 10), AG03199 (10 years, CCR, PDs 10). HGPS lymphoblastoid cell lines were AG03506 (13 years, CCR), AG03344 (10 years, CCR). Control fibroblast cell lines were AG08469 (38-year-old healthy male, CCR, PDs 4) and CRL-1474 (7 years, ATCC, PDs 12). The control lymphoblastoid cell line was AG03504 (41-year-old healthy female, CCR). Cells were grown in medium (Minimum Essential Medium (Gibco) for fibroblasts and RPMI (Gibco) for lymphocytes) supplemented with 15% fetal calf serum, 2 mM L-glutamine, 100 U/ml penicillin and 100 µg/ml streptomycin at 37 °C in 5% $CO_2$. Fibroblasts were analyzed over ≤30 population doublings while the cells maintained a constant growth rate with a typical doubling time of 48 h. Electroporations were carried out with a BTX electroporator ECM 830 (175 V, 1-ms pulse, five pulses, 0.5-s interval between pulses). Cells were electroporated in serum-free medium at ~$2 \times 10^7$ cells/ml (fibroblasts from one 75-cm² flask at 80–90% confluence in 100 µl) in a 2-mm-gap cuvette using either 5 µg plasmid DNA and 15 µg sheared salmon sperm carrier DNA, or the indicated amount of morpholino oligonucleotide without carrier DNA. Oligonucleotides were delivered in two or three rounds at 48-h intervals for fibroblasts and at 24-h intervals for lymphocytes. To prevent cell division, 24 h before treatment fibroblasts were either plated at 100% confluence or serum starved in 0.5% fetal calf serum. Contact inhibition and serum starvation were maintained throughout the treatment (two deliveries over 4 d). HeLa cells were grown in Dulbecco Modified Eagle Medium supplemented with 10% fetal calf serum, 2 mM L-glutamine, 100 U/ml penicillin and 100 µg/ml streptomycin at 37 °C in 5% $CO_2$.

**Phenotypic evaluation and statistical analysis.** To quantify changes in the cellular phenotype upon treatment, 200 cells were analyzed in each experiment for each parameter. Morphological abnormalities in the nucleus of control and HGPS cells were quantified based on contour ratio ($4\pi \times$ area/perimeter²) as described[6]. The contour ratio for a circle is 1. As the nucleus becomes more lobulated, this ratio approaches 0. Nuclei with contour ratios <0.7 were considered abnormal. The cellular levels of LAP2, lamin B, HP1α and Tri-Me-K9 in the nuclei of HGPS and control cells were quantified by imaging cells with identical settings and measuring the average intensity of the fluorescent signal in the entire nucleus using Metamorph software. The intensity from 20 control cells was averaged and used as reference to determine the fold reduction in every cell. Cells showing at least a twofold reduction were considered abnormal. Statistical significance of the differences in the percentage of abnormal cells was determined by contingency table analysis and $\chi^2$ test. To assess the phenotype of HGPS fibroblasts upon expression of wild-type lamin A, cells were fixed 24 h, 72 h or 10 d after transfection. To assess the phenotype of HGPS fibroblasts upon treatment with morpholino oligonucleotide, cells were fixed after three rounds of electroporation 7 d after the first delivery.

**Modified antisense oligonucleotide.** Morpholino oligonucleotides were purchased from Gene Tools. Exo11: 5′-GGGTCCACCCACCTGGGCTCCTGAG-3′. Control scrambled: 5′-GCTGCCACGTGACGTGGCAGCCTCC-3′.

*Note: Supplementary information is available on the Nature Medicine website.*

1. DeBusk, F.L. The Hutchinson-Gilford progeria syndrome. Report of 4 cases and review of the literature. *J. Pediatr.* **80**, 697–724 (1972).
2. Uitto, J. Searching for clues to premature aging. *Trends Endocrinol. Metab.* **13**, 140–141 (2002).
3. Eriksson, M. *et al.* Recurrent *de novo* point mutations in lamin A cause Hutchinson-Gilford progeria syndrome. *Nature* **423**, 293–298 (2003).
4. De Sandre-Giovannoli, A. *et al.* Lamin A truncation in Hutchinson-Gilford progeria. *Science* **300**, 2055 (2003).
5. Csoka, A.B. *et al.* Novel lamin A/C gene (*LMNA*) mutations in atypical progeroid syndromes. *J. Med. Genet.* **41**, 304–308 (2004).
6. Goldman, R.D. *et al.* Accumulation of mutant lamin A causes progressive changes in nuclear architecture in Hutchinson-Gilford progeria syndrome. *Proc. Natl. Acad. Sci. USA* **101**, 8963–8968 (2004).
7. Ye, Q., Callebaut, I., Pezhman, A., Courvalin, J.C. & Worman, H.J. Domain-specific interactions of human HP1-type chromodomain proteins and inner nuclear membrane protein LBR. *J. Biol. Chem.* **272**, 14983–14989 (1997).
8. Jenuwein, T. & Allis, C.D. Translating the histone code. *Science* **293**, 1074–1080 (2001).
9. Holt, I. *et al.* Effect of pathogenic mis-sense mutations in lamin A on its interaction with emerin *in vivo*. *J. Cell Sci.* **116**, 3027–3035 (2003).
10. Vaughan, A. *et al.* Both emerin and lamin C depend on lamin A for localization at the nuclear envelope. *J. Cell Sci.* **114**, 2577–2590 (2001).
11. Johnson, B.R. *et al.* A-type lamins regulate retinoblastoma protein function by promoting subnuclear localization and preventing proteasomal degradation. *Proc. Natl. Acad. Sci. USA* **101**, 9677–9682 (2004).
12. Sazani, P. & Kole, R. Therapeutic potential of antisense oligonucleotides as modulators of alternative splicing. *J. Clin. Invest.* **112**, 481–486 (2003).
13. Giles, R.V., Spiller, D.G., Clark, R.E. & Tidd, D.M. Antisense morpholino oligonucleotide analog induces missplicing of C-myc mRNA. *Antisense Nucleic Acid Drug Dev.* **9**, 213–220 (1999).
14. Summerton, J. Morpholino antisense oligomers: the case for an RNase H-independent structural type. *Biochim. Biophys. Acta* **1489**, 141–158 (1999).

15. Lin, F. & Worman, H.J. Structural organization of the human gene encoding nuclear lamin A and nuclear lamin C. *J. Biol. Chem.* **268**, 16321–16326 (1993).

16. Summerton, J. *et al.* Morpholino and phosphorothioate antisense oligomers compared in cell-free and in-cell systems. *Antisense Nucleic Acid Drug Dev.* **7**, 63–70 (1997).

17. Ly, D.H., Lockhart, D.J., Lerner, R.A. & Schultz, P.G. Mitotic misregulation and human aging. *Science* **287**, 2486–2492 (2000).

18. Csoka, A.B. *et al.* Genome-scale expression profiling of Hutchinson-Gilford progeria syndrome reveals widespread transcriptional misregulation leading to mesodermal/mesenchymal defects and accelerated atherosclerosis. *Aging Cell* **3**, 235–243 (2004).

19. Mounkes, L.C., Kozlov, S., Hernandez, L., Sullivan, T. & Stewart, C.L. A progeroid syndrome in mice is caused by defects in A-type lamins. *Nature* **423**, 298–301 (2003).

20. Moulton, H.M., Nelson, M.H., Hatlevig, S.A., Reddy, M.T. & Iversen, P.L. Cellular uptake of antisense morpholino oligomers conjugated to arginine-rich peptides. *Bioconjug. Chem.* **15**, 290–299 (2004).

21. Gebski, B.L., Mann, C.J., Fletcher, S. & Wilton, S.D. Morpholino antisense oligonucleotide induced dystrophin exon 23 skipping in mdx mouse muscle. *Hum. Mol. Genet.* **12**, 1801–1811 (2003).

22. Garcia-Blanco, M.A., Baraniak, A.P. & Lasda, E.L. Alternative splicing in disease and therapy. *Nat. Biotechnol.* **22**, 535–546 (2004).